Generation of Complex Motor Patterns in American Grasshopper via Current-Controlled Thoracic Electrical Interfacing

Susan L. Giampalmo, Benjamin F. Absher, W. Tucker Bourne, Lida E. Steves,
Vassil V. Vodenski, Peter M. O'Donnell, and Jonathan C. Erickson

Abstract— Micro-air vehicles (MAVs) have attracted attention for their potential application to military applications, environmental sensing, and search and rescue missions. While progress is being made toward fabrication of a completely human-engineered MAV, another promising approach seeks to interface to, and take control of, an insect's nervous system. Cyborg insects take advantage of their innate exquisite locomotor, navigation, and sensing abilities. Recently, several groups have demonstrated the feasibility of radio-controlled flight in the hawkmoth and beetle via electrical neural interfaces. Here, we report a method for eliciting the "jump" response in the American grasshopper (*S. Americana*). We found that stimulating the metathoracic T3 ganglion with constant-current square wave pulses with amplitude 186 ± 40 μA and frequency 190 ± 13 Hz reproducibly evoked ($\geq 95\%$ success rate) the desired motor activity in N=3 test subjects. To the best of our knowledge, this is the first report of an insect cyborg with a synchronous neuromuscular system.

I. INTRODUCTION

Within the past decade, understanding and ability in the fields of neuroscience, physiology, and engineering have reached a point such that their fusion has realistic and widespread applicability [1]. One of these interdisciplinary investigations, the interfacing of an electronic driver with an animal's nervous system to create a cyborg, seeks to harness the animal's specialized navigational capacities and locomotor functions. Such abilities include the generation of two to three times more lift than conventional aerodynamics, execution of high velocity turns [2], ability to sense polarization of light and directional hearing into the ultrasound range (10 kHz above 45 dB) [3]. While substantial progress is being made toward development of purely mechanical micro-air vehicles (MAVs)—such as magnetic induction vibrational energy harvesting devices [4], and fabrication of light-weight polyester thin film wings with inlaid carbon-fiber venation acting as a support framework [5]—significant challenges remain. Engineering a cyborg insect alleviates several challenges facing the development of purely mechanical MAVs, namely the time required imitating biological structures, and energetic requirements constrained by fuel density [1]. Proposed uses for cyborgs range from to military applications, to search-and-rescue aids, to ecosystem monitors [6].

Various methods have been used to create insect cyborgs. Bozkurt et al. developed Early Metamorphosis Insertion Technology (EMIT), placing electronics in the pupal stage of the tobacco hawkmoth *M. sexta* [7]. In mature moths, stimulation of electrode in-flight muscles resulted in ipsilateral down- and up-stroke actuation, providing directional control of flight. Tsang et al. used EMIT to implant directly into the CNS nerve cord; stimulation altered abdominal positioning influencing flight direction of tethered adult moths. Increased magnitude of such movements correlated with increase in voltage or pulse frequency [8]. Recently, Sato and Maharbiz et al. demonstrated remote-controlled free flight in the beetle *Mecynorrhina torquata* [6]. They used stainless steel microelectrodes to stimulate the base of optical lobe interneurons. 100 Hz pulses of median 3.2 V amplitude reproducibly initiated flight; a higher frequency pulse resulted in cessation of flight. Directionality was achieved via electrodes stimulating the lateral basal muscles [6].

Motivated by these previous works, we sought to test the applicability of such electronic neural interfacing on *Schistocerca Americana*, the American grasshopper. Use of *S. Americana* was founded in the local availability and size (potential payload capacity), as well as extensively researched neurobiology—the majority pertaining to the thoracic ganglia's control of hind legs, flight, and ventilation [3]. We sought to reliably generate the complex motor function of jumping, with limited impairment to the grasshopper.

Jumping is used as an escape response, away from threatening stimuli, and for rapid locomotion during the flightless juvenile stage. A catapult-like motion results from the contraction and relaxation of antagonistic muscles, in a cycle of cocking, co-contractions, and triggering. During cocking, front legs are placed symmetrically and hind legs depressed into crouch by contraction of the flexor. The co-contraction of the extensor stores force. Inhibition triggering relaxation of the flexor allows the extensor to produce a rapid and powerful extension of legs into the jump. This sequence of events is a function of the motor neurons firing rate, muscles contracting rate, and communication of interneurons.

S. Americana have a synchronous neuromuscular system, characterized by a one-to-one ratio of neural activity (action potentials) and muscle contractions [3]. The neuromuscular activity leading to a jump is coordinated by the T3 metathoracic ganglion [3] (see Fig. 1, bottom-left). Hind legs are innervated by three common inhibitory motor neurons and 70 excitatory motor neurons [9]. As the isolated metathoracic ganglion can generate the entire jump motor sequence [10],

all interneuron output channels must be contained within this ganglion. Hence, we reasoned that stimulation of T3 metathoracic ganglion would provide necessary and sufficient output to stimulate the jumping motor pattern while minimally perturbing other sensory processes which would be vital for our cyborg's effectiveness.

Herein, we report a method for successfully eliciting the jump response with high reproducibility (>95%) via a current-controlled electrical interface to the T3 ganglion.

II. METHODS

S. Americana were captured in Lexington, Virginia and surrounding Rockbridge County, Virginia, USA during the month of October. Test subjects were stored in a terrarium at room temperature ($\approx$23 C) and ambient humidity ($\approx$40%), and fed a diet of leafy greens sprayed with mist daily for the duration of experimentation. To prepare subject for electrode insertion, activity was decreased by confinement in an ice-lined cooling chamber. A loose embroidery floss "leash", designed to minimize contact with mechanosensory receptors, was secured between the first and second pair of legs, across the T2 region (Fig. 1, top-right). The leash length was sufficient so as not to interfere with the range of jump. The subject was then placed in a channel created within a compacted bag of ice, to maintain an inactive state during the electrode insertion (Fig. 1, top-left).

To insert electrodes, small incisions were made with a scalpel, using the ventral cuticle pattern as a template (Fig. 1, bottom-left and bottom-right). The active electrode was inserted into the metathoracic T3 ganglion. The counter electrode was inserted several millimeters proximal to the stimulus electrode to allow current to flow through an already established pathway. Electrodes (stainless steel, 125 μm dia.) were secured with a small amount of super-glue. The length of the stainless steel conductor ($\approx$2 m) was insulated with electrical tape to prevent shorting the leads, which would sometimes come into contact due to grasshopper motor activity. Test subjects were allowed to return to room temperature ($\approx$25 C) and normal activity level prior to electrical stimulation.

We opted for constant-current stimuli, eliminating the exponential decay with RC time constant that would vary between test subjects due to the passive electrical impedance. Square-pulse analog voltage waveforms with variable amplitude, frequency, number of pulses, and duty cycle were produced with a National Instruments 6251 PCI hardware. Parameter values were set via a custom-programmed LabView interface. To convert voltage pulses into current pulses, we built an op-amp based V→I converter (Fig. 2, modified from the original design presented in [11]. Fig 3 illustrates the command waveform delivered to the V→I converter (yellow trace), as well as the resulting voltage that develops on the active electrode (blue trace). Note that the exponential charging/discharging of the electrode voltage is to be expected, assuming that the metal-electrolyte interface of the electrode coupled to the interstitial milieu acts as a capacitor in series with a bulk resistance [12].

Fig. 1. **Top-left**: Test subject prepared for electrode implantation after being inactivated on ice. **Top-right**: Test subject post-electrode insertion and leash attachment. One uninsulated conductor lead is seen trailing off to background, and embroidery floss leash trails off to foreground of photo. **Bottom-right:** Making incisions through ventral cuticle with scalpel. **Bottom-left:** Anatomical landmarks. a = prostemal spine; b = metathoracic ganglion; c = mesosternal lobe d = metasternal lobe.

Square-pulse parameter ranges tested were as follows: Amplitude = 10 – 250 μA; Frequency = 1 – 225 Hz; Number of pulses = 10–100; Duty cycle = 50%. Actual values tested focused on a particular range once successful jumps were elicited from one subject.

Six subjects were tested using this paradigm. (Additionally, we tested three other stimulation paradigms; see Discussion). In order to accurately quantify the quality of jump response, a graded Response Scale Qualitative (RSQ) was developed, with 0 being assigned for no response and 7 being assigned for a fully executed motor sequence. Table I describes the score assigned to each class of response.

III. RESULTS

With appropriate parameters for amplitude and frequency, a $\geq$ 95% successful jump rate (RSQ=7) was produced in 3 out of 6 test subjects (19/20, 23/25, and 37/38 trials, respectively). A supplementary video available at `http://home.wlu.edu/~ericksonj/cyborgGrasshopper.MOV` demonstrates the typical jumping behavior observed. No detrimental effects on grasshopper health, behavior, or natural motor activity were noted 24 hrs after testing. Additionally, we elicitied a successful jump response during a second testing period, 24 hrs
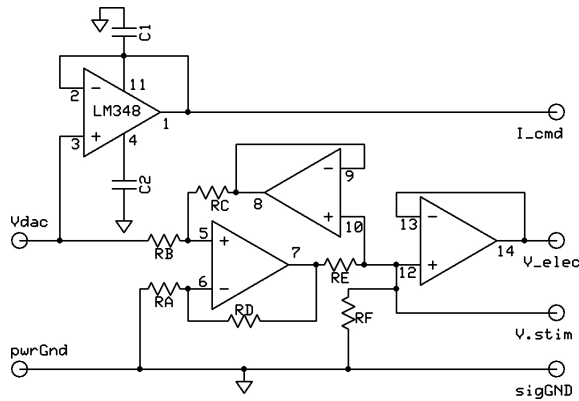
Fig. 2. Voltage to current converter. The NI 6251 DAC analog waveform drives the input, $Vdac$, with an amplitude range of 0–10 V. R_E = 20 kΩ defines the output current as $I = Vdac/R_E$, with a range of 0–500 μA. The outputs $V.stim$ and $sigGND$ drive the active and counter electrodes, respectively. The output from the buffers provide readouts of the command voltage I_cmd, and resulting electrode potential V_elec. Op-amp is 4/4 LM348 (Texas Instruments). Decoupling capacitors C_1 and C_2 are 0.1 μF. R_F = 6.8 MΩ; all other resistors are 150 kΩ.
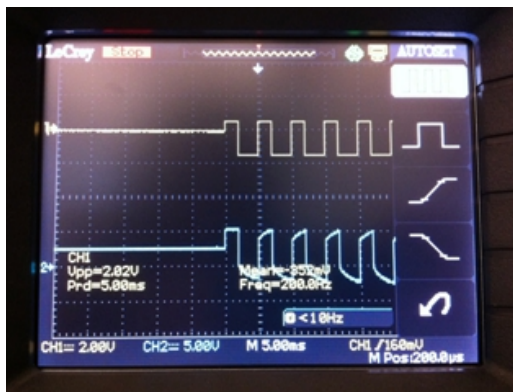

Fig. 3. Illustration of command waveform from NI PCI 6251 which drives the voltage-to-current converter (yellow trace), and resulting time-course of electrode voltage (blue trace).

Scale	Response
0	No response
1	Generalized physical response; any behavioral/physical change resulting from stimulation
2	Poorly defined physical response localized to thoracic region
3	Defined movement of single hind leg; sharp twitch or kick, no net displacement of body
4	Defined and coordinated movement of hind legs; sharp twitch or kick, no net displacement of body
5	Defined and coordinated movement of hind legs, correct body positioning; sharp twitch or kick, no net displacement of body
6	Flawed yet defined and coordinated movement of hind legs producing net displacement of body, but typically incomplete motor sequence
7	Successful jump: correct/fully executed motor sequence

TABLE I

RESPONSE SCALE QUALITATIVE (RSQ) SCORE SUMMARY

after the initial successful test, in the one subject examined in this manner.

Table II summarizes the effective stimulation parameters for each test subject. The mean test parameters that initiated the jump response were as follows: Current amplitude = 186 $\pm$ 40 μA; Frequency = 190 $\pm$ 13 Hz; Number of pulses = 43.3 $\pm$ 6.1 pulses.

Subject	V (Volts)	I (μA)	f (Hz)
1	2.89	144.5	192
2	4.5	225	200
3	3.75	187.5	175
Mean $\pm$ S.D	3.7 $\pm$ 0.8	186 $\pm$ 40	190 $\pm$ 13

TABLE II

PARAMETER VALUES FOR COMMAND VOLTAGE, CURRENT AMPLITUDE AND FREQUENCY WHICH EVOKED SUCCESSFUL JUMP RESPONSES.

As Fig. 4 shows, there was a strong dependence of the motor response on both amplitude and frequency of the command pulses. Above and below the range the 185 $\pm$ 40 μA current range, RSQ values sharply fell. While the data is suggestive of a similar correlation for the frequency above and below 189.0 $\pm$ 12.8 Hz, more testing is needed to verify this is the case.
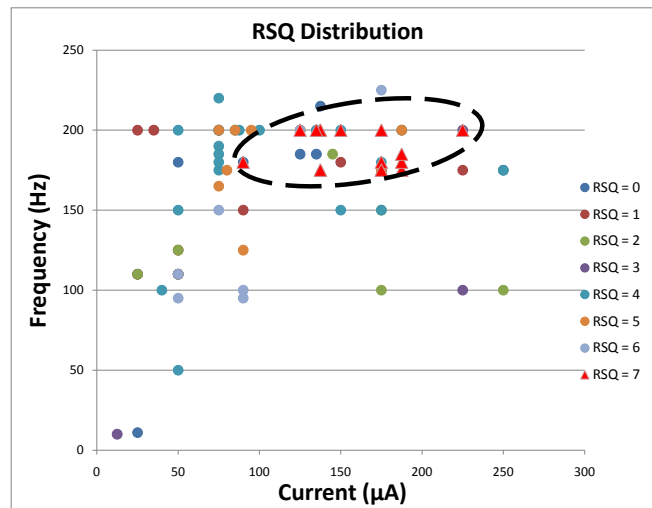

Fig. 4. Response quality depends on amplitude and frequency of electrical stimulation. The dashed oval highlights the parameter ranges for amplitude and frequency that successfully elicited the jump response (RSQ = 7).

Regarding the 3 test subjects in which we failed to generate motor activity, 2 died several days after the electrode implantation and before testing, probably due to dehydration while isolated in a separate storage chamber; and 1 subject's hind leg unexpectedly detached at the beginning of the electrical stimulus test period, probably due to the fact that the femoral joint can be relatively weak depending on the developmental stage [3].

IV. DISCUSSION

To the best of our knowledge, this is the first demonstration of controlled locomotion via neural interface in an insect with

a synchronous neuromuscular system. The current/voltage range that produced successful jumps is highly similar to the range of values noted to trigger flight in other insect cyborg experiments. By contrast, the frequencies required to initiate a jump were higher than those used to initiate flight by a factor of 2–10. Specifically, Bozkurt et al. used a 3.5 V_{pp}, 20 Hz antennal lobe stimulation for flight in hawkmoth [7]. Sato et al. observed that 3–4 V voltage pulses delivered at 100 Hz triggered flight bouts in beetles [6].

The exact neural pathways stimulated to evoke the observed grasshopper jump response are not known. A control experiment (N=1), where the active electrode was inserted through the mesosternal plate, rostral to the T3 ganglion, failed to elicit any motor response. This observation suggests that we were in fact stimulating the T3 ganglion motor neurons.

In all, we tried four different methods of stimulation, which had varying degrees of success. Metathoracic stimulation, the method described in detail herein, produced the most consistent results. Using additional test subjects, we also tried stimulating the base of the optic lobes (N=10) in a manner similar to that described in [6]. Curiously, this method failed to initiate any coordinated motor activity in *S. Americana* beyond rapid twitching and/or rotation of the hind legs. This difference in outcomes may be due to the fact that flight muslces in most beetles, including *M. torquata*, are asynchronous: A single episode of neural activity can lead to sustained oscillatory muscular activity [13]. Therefore, we speculate that driving the beetle's optic lobe may produce a low yet sufficient level of neural output to trigger sustained flight muscle activity, whereas doing so in the grasshopper may lead to a sub-threshold (low-frequency, short time duration) neural response which is incapable of driving synchronous femoral muscle activity. Synaptic integration in the CNS is complex; stimulating the T3 ganglion is a more "direct-drive" approach.

The third method we tested, direct muscle stimulation, involved inserting the electrodes directly into the hind-leg extensor muscle (N=8). Some precisely timed, rapid twitch-like motions were generated, but never a jump response. One issue encountered with this method was the limited current range available: too high a command current ($\geq$ 50 μA) often caused the hind leg to detach, probably due to generating excessive contractile force. Finally, we tested ovipositor stimulation (N=3), which entailed inserting the active electrode at the pronotum and the ground electrode a few mm into the ovipositor (aboral terminal orifice of the abdomen). This resulted in consistent motor reaction in 2 test subjects, but in the form of irritated walking rather than actual jumping. We hypothesize this result is due to a general activation of the ventral nerve cord, as current would primarily flow along the axis parallel to it.

V. FUTURE WORK

Histological preparations are currently being examined to more precisely determine where electrodes were positioned relative to the metathoracic ganglia. Future work will include systematic blind testing of stimulus parameters in more test subjects to further establish generality of the results obtained thus far. Improvements for all stimulation methods include allowing for an acclimation period following electrode implantation (e.g., [7]), and establishing a climate-controlled testing environment. We plan to investigate methods of controlling directional heading. One approach involves evaluating simultaneous delivering of sensory stimuli (e.g., light and air puffs) with electrical stimuli. We also plan investigate methods to miniaturize electrodes (e.g., [14]) and control circuitry for a remote-controlled interface.

VI. ACKNOWLEDGMENTS

REFERENCES

[1] M. Maharbiz and H. Sato, "Cyborg Beetles," *Scientific American Magazine*, vol. 303, no. 6, pp. 94–99, 2010.

[2] C. Ellington, "The novel aerodynamics of insect flight: applications to micro-air vehicles." *The Journal of Experimental Biology*, vol. 202, no. Pt 23, p. 3439, 1999.

[3] M. Burrows and I. NetLibrary, *The neurobiology of an insect brain*. Oxford University Press Oxford, 1996.

[4] C. S.C., Y. F.M., D.-G. A., O. F., O. D.M., and L. J.H., "Harvesting energy from moth vibration during Flight," *Proc. Power MEMS*, pp. 313–325, 2009.

[5] J. Shang, S. Combes, B. Finio, and R. Wood, "Artificial insect wings of diverse morphology for flapping-wing micro air vehicles," *Bioinspiration & biomimetics*, vol. 4, p. 036002, 2009.

[6] H. Sato, C. Berry, Y. Peeri, E. Baghoomian, B. Casey, G. Lavella, J. VandenBrooks, J. Harrison, and M. Maharbiz, "Remote radio control of insect flight," *Frontiers in integrative neuroscience*, vol. 3, 2009.

[7] A. Bozkurt, R. Gilmour, and A. Lal, "Balloon-assisted flight of radio-controlled insect biobots," *Biomedical Engineering, IEEE Transactions on*, vol. 56, no. 9, pp. 2304–2307, 2009.

[8] W. Tsang, Z. Aldworth, A. Stone, A. Permar, R. Levine, J. Hildebrand, T. Daniel, A. Akinwande, and J. Voldman, "Insect flight control by neural stimulation of pupae-implanted flexible multisite electrodes," in *12th Int. Conf. Miniaturized Systems for Chemistry and Life Sciences (TAS 2008)*, 2008.

[9] M. Siegler and C. Pousman, "Distribution of motor neurons into anatomical groups in the grasshopper metathoracic ganglion," *The Journal of Comparative Neurology*, vol. 297, no. 2, pp. 313–327, 1990.

[10] S. Ryckebusch and G. Laurent, "Rhythmic patterns evoked in locust leg motor neurons by the muscarinic agonist pilocarpine," *Journal of neurophysiology*, vol. 69, no. 5, p. 1583, 1993.

[11] D. Wagenaar and S. Potter, "A versatile all-channel stimulator for electrode arrays, with real-time control," *Journal of neural engineering*, vol. 1, p. 39, 2004.

[12] D. Robinson, "The electrical properties of metal microelectrodes," *Proceedings of the IEEE*, vol. 56, no. 6, pp. 1065–1071, 1968.

[13] R. Josephson, J. Malamud, and D. Stokes, "Asynchronous muscle: a primer," *Journal of Experimental Biology*, vol. 203, no. 18, p. 2713, 2000.

[14] W. Tsang, A. Stone, Z. Aldworth, D. Otten, A. Akinwande, T. Daniel, J. Hildebrand, R. Levine, and J. Voldman, "Remote control of a cyborg moth using carbon nanotube-enhanced flexible neuroprosthetic probe," in *Micro Electro Mechanical Systems (MEMS), 2010 IEEE 23rd International Conference on*. IEEE, 2010, pp. 39–42.